AIMS Energy, 12(2): 439–463.
DOI: 10.3934/energy.2024020
Received: 19 November 2023
Revised: 15 February 2024
Accepted: 26 February 2024
Published: 15 March 2024

http://www.aimspress.com/journal/energy

Research article

Forecasting mixture composition in the extractive distillation of n-hexane and ethyl acetate with n-methyl-2-pyrrolidone through ANN for a preliminary energy assessment

Daniel Chuquin-Vasco[1,*], Dennise Chicaiza-Sagal[2], Cristina Calderón-Tapia[3], Nelson Chuquin-Vasco[4], Juan Chuquin-Vasco[4] and Lidia Castro-Cepeda[5]

[1] Escuela Superior Politécnica de Chimborazo (ESPOCH), Chemical Engineering Career, Safety, Environment and Engineering Research Group (GISAI), Riobamba, Chimborazo, Ecuador
[2] SOLMA, Advanced Mechanical Solutions, Mechanical Engineering and Construction Services, Quito, Pihincha, Ecuador
[3] Escuela Superior Politécnica de Chimborazo (ESPOCH), Environmental Engineering Career, Riobamba, Chimborazo, Ecuador
[4] Escuela Superior Politécnica de Chimborazo (ESPOCH), Mechanical Engineering Career, Safety, Environment and Engineering Research Group (GISAI), Riobamba, Chimborazo, Ecuador
[5] SOLMA, Advanced Mechanical Solutions, Mechanical Engineering and Construction Services, Quito, Pichincha, Ecuador

* **Correspondence:** Email: daniel.chuquin@espoch.edu.ec; Tel: +593998163018.

Abstract: We developed an artificial neural network (ANN) to predict mole fractions in the extractive distillation of an n-hexane and ethyl acetate mixture, which are common organic solvents in chemical and pharmaceutical manufacturing. The ANN was trained on 250 data pairs from simulations in DWSIM software. The training dataset consisted of four inputs: Feed flow inlet (T1-F), Feed Stream Mass Flow temperature pressure (FM1-F), Make-up stream mass flow (FM2-MU), and ERC tower reflux ratio (RR-ERC). The ANN demonstrated the ability to forecast four output variables (neurons): Mole fraction of n-hexane in the distillate of EDC (XHE-EDC), Mole fraction of N-methyl-2 pyrrolidone in the bottom of EDC (XNMP-EDC), Mole fraction of ethyl acetate in the distillate of ERC (XEA-ERC), and Mole fraction of N-methyl-2 pyrrolidone in the bottom of ERC (XNMP-ERC).The ANN architecture contained 80 hidden neurons. Bayesian regularization training yielded high prediction accuracy (MSE = 2.56×10^{-7}, R = 0.9999). ANOVA statistical validation indicated that ANN could reliably forecast mole fractions. By integrating this ANN into process control systems, manufacturers could enhance product quality, decrease operating expenses, and mitigate composition variability risks. This data-driven modeling approach may also optimize energy consumption when combined with genetic algorithms. Further research will validate predictions onsite and explore hybrid energy optimization technologies.

Keywords: ANN; DWSIM; ethyl acetate; extractive distillation; n-hexane

1. Introduction

Ethyl acetate and n-hexane are two extensively utilized organic solvents. However, the separation of their mixtures poses a challenge due to the formation of a homogeneous minimum-boiling azeotrope with 65.7 mol% n-hexane at 64.85 ℃ and 1 atm [1]. In order to separate such mixtures that contain azeotropes or exhibit low relative volatility, non-conventional distillation technologies, including azeotropic distillation, pressure-swing distillation (PSD), and extractive distillation (ED), have been widely employed [1,2].

The existence of azeotropes in binary mixtures inhibits the efficient separation of individual components through conventional distillation methods. Consequently, various specialized distillation techniques have been developed, including extractive distillation (ED), pressure oscillation distillation (PSD), azeotropic distillation (AD), thermally coupled extractive distillation (TCED), and extractive dividing wall columns (EDWC), among others [3].

ED is widely recognized as a dominant technology for the separation of mixtures containing azeotropes, utilizing a carryover agent. The field of extractive distillation has witnessed significant advancements over the past two decades. Through extractive distillation, azeotropic mixtures with low relative volatility can be effectively separated, employing various types of carrier agents such as light, heavy, or those with intermediate boiling points. These agents can be in the form of heterogeneous and homogeneous solvents, classic solvents, ionic liquids, or deep eutectic solvents [4].

Iqbal et al. [5] conducted a study exploring different methods for the separation of mixtures, including pressure oscillation distillation (PSD), extractive distillation (ED), and azeotropic distillation (AD). Their findings indicate that ED is the most economically efficient method, as it exhibits a cost reduction of 27.62% compared to batch distillation with pressure oscillation in a binary mixture of dichloromethane-methanol. Similarly, Zhu et al. [6] concluded that ED is capable of achieving a separation efficiency of up to 99.99% by mole for components within ethyl-cyclohexane mixtures. Additionally, they propose the incorporation of a two-stage preheating process to enhance energy utilization and achieve cost reduction. The results demonstrate that the total annual cost (TAC) of the ED process is 58.2% lower than that of PSD and the two-stage process. The focus of this study is to establish an efficient separation technique for an ethyl acetate and cyclohexane system, which holds significant importance for the pesticide industries.

1.1. Simulation of distillation processes for n-hexane and ethyl acetate system

Yang and Ward [7] conducted a study on the separation of n-hexane and ethyl acetate using a pressure change distillation (PSD) process. This particular process is advantageous as it does not introduce any additional components into the system, known as cargoes. However, the results revealed that the total annual cost (TAC) of this PSD process amounted to 2.14 million dollars, which is higher compared to other carry-based separation processes that range from 0.92 to 1.76 million dollars.

In a study by Lü et al. [8], a comparison was made between different distillation methods for the azeotropic mixture of n-hexane and ethyl acetate. The optimized pressure change distillation (PSD) was compared to the continuous homogenous azeotropic distillation (CHAD) processes, which utilized acetone as a carrier and distillation agent. The researchers used integrated pressure oscillation (HIPSD) and found that partial HIPSD was more favorable for mixtures of ethyl acetate and n-hexane, as it

resulted in energy cost reduction and lower TAC compared to the CHAD process. The reduction in TAC was 62.61% and 49.26% when compared to the CHAD process, and 40.79% and 35.94% when compared to the conventional PSD. This reduction can be attributed to the fact that the reboiler of the low pressure column (LPC) consumes energy from the overhead steam of the high pressure column (HPC) instead of low pressure steam. Additionally, this process offers advantages such as avoiding product contamination, energy savings, and overall economic benefits.

Li et al. [9] proposed the use of heterogeneous azeotropic distillation (HAD) for a ternary system consisting of acetonitrile/ethyl acetate/n-hexane. To minimize energy consumption, they incorporated a heat pump based on optimal heterogeneous azeotropic distillation, which utilized heat integration technology to enhance energy recovery. The results showed that the combination of the heat pump with the highest preheating temperature (HPT) assisted by the HAD process, along with heat integration, resulted in better performance in terms of economic, environmental, energy, and exergetic aspects compared to conventional HAD processes. This improvement led to a reduction of 52.17% in TAC, 68.86% in energy consumption, 65.87% in gas emissions, and 64.46% in the destruction of exergy.

1.2. ANN as a prediction tool in chemical industries

The artificial neural network has the capability to approximate any nonlinear mapping through the process of learning, enabling its application in the identification and modeling of nonlinear systems without being limited by a specific nonlinear model. Its fault tolerance is demonstrated by its ability to continue overall activities even in the presence of system components' failures. Artificial intelligence based on neural networks possesses recognition, classification, error correction, and time series retention capabilities [10–16].

The application of artificial neural networks (ANNs) in the chemical industry has facilitated the development of novel methodologies for addressing operational and process optimization challenges through the prediction of outcomes derived from process simulation databases. Various networks with different structures have been employed for machine learning and can be classified into supervised and unsupervised categories [17].

In a study by Yazdizadeh et al. [18], a three-layer ANN was utilized to predict the final concentration of furfural produced in the presence of $NaHSO_4$ + H_2SO_4 in a reactor. Input variables for the ANN included reactor temperature, pressure, reaction time, H_2SO_4 level, and bagasse humidity. The optimal process conditions were determined as 160 ℃, 8 bar, and 23% sulfuric acid, resulting in a furfural yield of 97.4%.

Esonye et al. [19] optimized biodiesel production from Sweet Almond using response surface methodology (RSM) and artificial neural networks (ANNs) through oil transesterification with sodium hydroxide. The optimization variables included temperature, catalyst concentration, reaction time, and the oil/methanol molar ratio. The study concluded with biodiesel yields of 94.36% from RSM and 95.45% from ANN models, both achieved at a catalyst concentration of 1.5% w/w, a reaction time of 65 minutes, a 1:5 oil/methanol molar ratio, and a temperature of 50 ℃. ANN model statistics indicated a mean squared error of 6.005, mean absolute error (MAE) of 2.786, and mean absolute deviation of 1.893.

Ge et al. [20] proposed a convolutional neural network (CNN) for the detection and diagnosis of faults in complex processes, using reactive distillation (RD) in the formic acid synthesis process as a reference. Different CNN configurations were tested and trained using MATLAB, with the best-performing network achieving a precision of 91.31%, comprising three convolutional layers, two pooling layers, and two fully connected layers.

Araújo et al. [21] applied neural networks to implement intelligent control systems for disturbance rejection in an extractive distillation column used for anhydrous ethanol production with ethylene glycol as a solvent. The control system, based on ANN, demonstrated a 99.5% accuracy in rejecting all disturbances while maintaining product specifications.

Inyang and Lokhat [22] conducted a comparative study between response surface methodology (RSM) and experimental modeling using an artificial neural network (ANN) for the recovery of propionic acid through extractive distillation. The results revealed that the composition of the extractant significantly influenced extraction efficiency, with experimental results closely aligning with the ANN-predicted value of 83.68%, indicating the superior predictive efficacy of the ANN methodology.

We are motivated by the notable absence of prior research utilizing artificial neural networks (ANNs) for predictive purposes in the specific context of Extractive Distillation for Separating n-hexane and ethyl acetate. The lack of previous investigations underscores the novelty and importance of applying ANN methodologies to this industrial process. Harnessing the predictive capabilities of neural networks in extractive distillation has the potential to enhance efficiency, optimize operational parameters, and provide valuable insights into the separation of n-hexane and ethyl acetate.

2. Materials and methods

2.1. Process description

Figure 1 illustrates the alternative extractive distillation process for separating to efficiently separate the mixture of n-hexane (HE) and ethyl acetate (EA) using N-methyl-2 pyrrolidone (NMP) as entrainer, adapted from [1]. In this process, the overhead vapor stream from the Extractive Distillation Column (EDC) is preheated using the EDC reboiler's condensate and then compressed by a compressor. The compressed overhead vapor, at higher temperature and pressure, is used to provide most of the heat duty for the EDC reboiler by releasing latent heat. The resulting condensate is initially used to preheat the overhead vapor stream. Later, its pressure is reduced to match the operating pressure of the EDC reflux drum, and it is further cooled using cooling water before being directed into the reflux drum.

In the process, a vapor recompression heat pump (VRHP-ED) is employed. The feed is introduced into the middle section of the EDC after preheating by the recovered recycle stream. Chilled NMP is fed to the upper section of the EDC. After mixing the two makeup streams and recycled NMP, high-purity n-hexane is obtained at the top of the EDC, while a mixture of ethyl acetate and NMP is collected at the bottom of the EDC, which is then fed to the recovery column (ERC). In ERC, high-purity ethyl acetate distillate is obtained, and NMP is recovered from the bottom.

The feed flow entering the Extractive Distillation Column (EDC) consists of a mixture containing 0.61 n-hexane (HE) and 0.39 ethyl acetate (EA) in a total amount of 100 kmol/h. The objective is to achieve a product purity, comprising EA and HE, of at least 0.99. The feed stream temperature is maintained at 25 ℃. Subsequently, the feed is preheated to 64 ℃ after passing through the reboiler of the recycling column at the bottom of EDC. This temperature of 64 ℃ matches the saturation temperature of the fresh feed at 1 atm pressure. The EDC operates at a pressure of 1 atm, following industrial practices to ensure operational flexibility and process safety. Additionally, a minimum temperature difference of 10 ℃ is selected as the criterion for all heat exchangers, including the reboilers and condensers, to provide sufficient driving force for heat transfer. Table 1 summarizes the composition of the feed entering the extractive column EDC, the study considered parameters such as pressure, temperature, molar flow rates of streams, and mole fractions of components. Tables 2–3 provide detailed operating conditions for the extractive (EDC) and recovery (ERC) columns, respectively. Additionally, Table 4 finally outlines the operating conditions of the compressor used in

the recompression stage. In the EDC, the distillate product is high-purity n-hexane (0.999), while the bottom product is a mixture of NMP (0.715) and ethyl acetate (0.285). In the ERC, the high-purity distillate product is ethyl acetate (0.999), and high-purity NMP (0.999) is obtained in the bottom stream.

Table 1. Feed conditions to Extractive Distillation Column (EDC).

Inlet	Parameter	Quantity	Unit
Feed Pre-heater	Pressure	1.2	atm
	Temperature	34	C
	Feed base (molar flow)	100	*K*mol/h
	Initial composition of EA ($C_4H_8O_2$)	0.39	-
	Initial composition of HE (C_6H_{14})	0.61	-
	Initial composition of NMP (C_6H_7NO)	0	-
NMP mix	Pressure	0.33	bar
	Temperature	101	C
	Make - up (molar flow)	90.88	Kmol/h
	Initial composition of EA ($C_4H_8O_2$)	0.05	-
	Initial composition of HE (C_6H_{14})	0	-
	Initial composition of NMP (C_6H_7NO)	0.95	-

*Note: Source: [1].

Table 2. Operating conditions of the Extractive Distillation Column (EDC).

Parameter	Quantity	Unit
Pressure	1	atm
# Column stages*	29	-
# Feed stage*	19	-
# Make-up stage*	5	-
Reflux ratio (RR1)	0.79	-
Feed molar flow	100	Kmol/h
Make-up molar flow	0.00389	Kmol/h
Condenser duty	224.50	kW
Reboiler duty 1	138.68	kW
Reboiler duty 2	856.75	kW
Cooler	76.80	kW
Pre-heater	218.30	kW

*Note: Numbered from the top of the distillation tower.
Source: [1].

Table 3. Operating conditions of the recovery column (ERC).

Parameter	Quantity	Unit
Pressure	1	atm
# Column stages*	9	-
# Feed stage, B1*	5	-
# Solvent inlet stage*	5	-
Reflux ratio (RR2)	0.26	-
Feed molar flow (B1)	124.32	Kmol/h
Condenser duty	468.84	kW
Reboiler duty	607.88	kW

*Note: Numbered from the top of the distillation tower.
Source: [1].

Table 4. Operating conditions of the compressor.

Parameter	Quantity	Unit
Inlet pressure	1	atm
Outlet pressure	4.77	atm
Compressor efficiency	0.8	-
Engine efficiency	0.9	-

*Note: Numbered from the top of the distillation tower.
Source: [1].

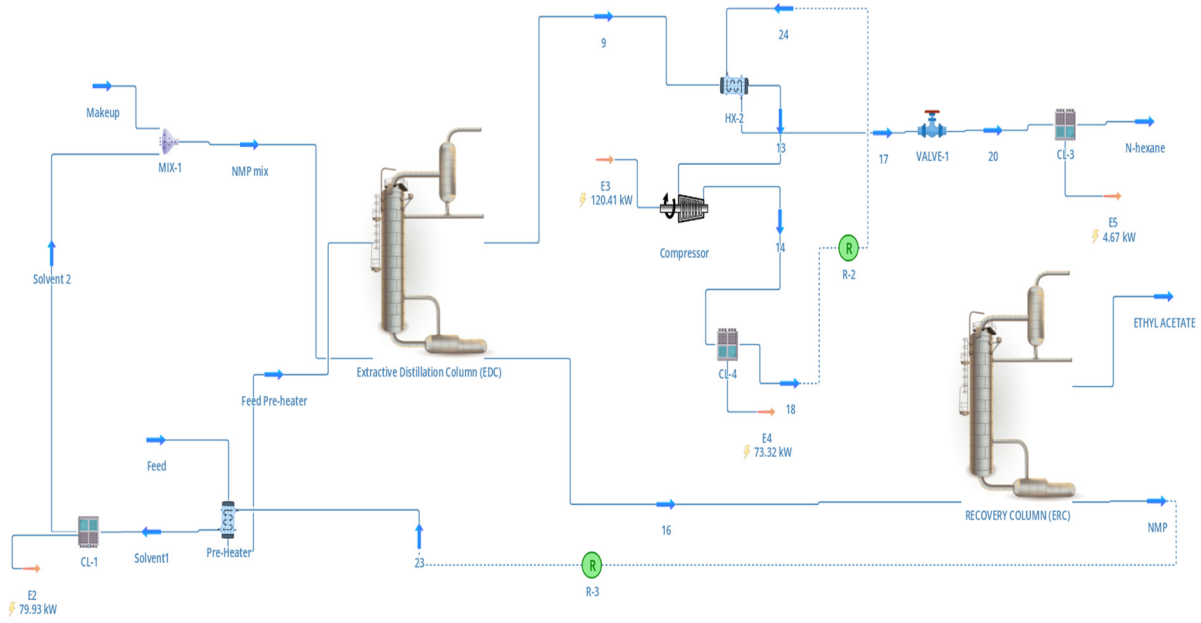

Figure 1. Simulation of the extractive distillation assisted by vapor recompression.

2.2. Methodology

Figure 2 delineates the methodical procedure employed for the development of the Artificial Neural Network (ANN). In its initial stage, the simulation and validation of the process explicated in Figure 1 is conducted, taking into account the operating conditions outlined in Tables 1–4. Subsequently, the ANN is formulated and verified, considering the inputs and outputs, as well as the constraints specified by the simulation. Finally, the functionality and predictive capacity of the ANN is evaluated through a graphic and statistical analysis.

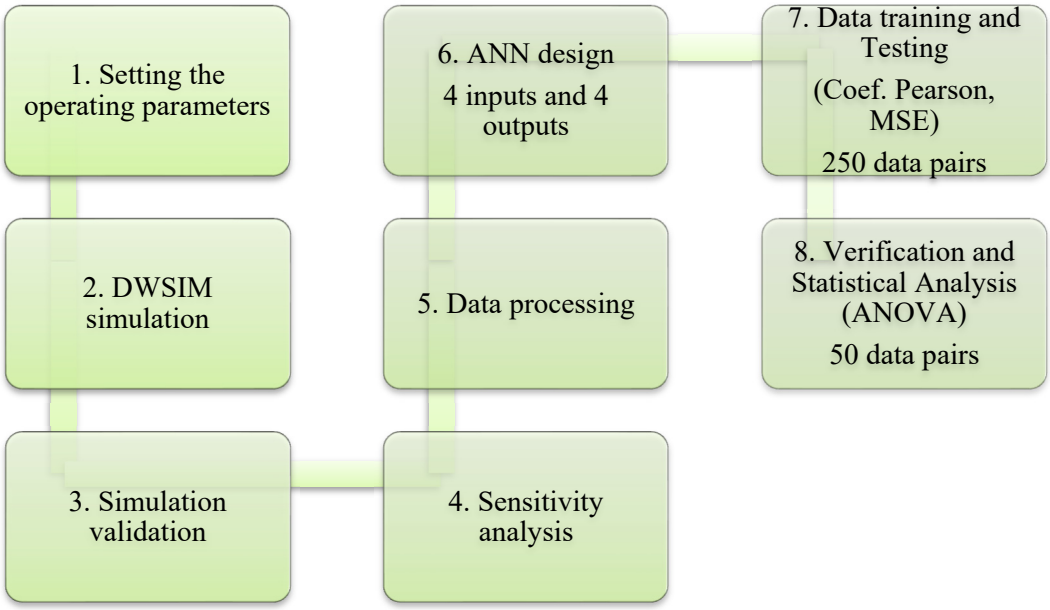

Figure 2. Methodological scheme of the designed ANN.

2.3. DWSIM simulation

DWSIM, a chemical process simulator that is open-source, can be accessed on various operating systems such as Windows, Linux, Android, macOS, and iOS. This software empowers engineers to effectively design process plants by employing rigorous thermodynamics principles and employing unit operations [23,24].

The distillation columns employed in the simulation presented in Figure 1 are representative of the "ChemSep Column" model. The flow streams are configured to utilize the Wilson properties package, while the distillation columns are customized to employ the DECHEMA/UNIFAC/Antoine thermodynamic models. These models are among the most extensively applied packages for the binary n-hexane/ethyl acetate system, capable of predicting phase equilibrium and various thermodynamic properties for a diverse range of systems [1,25–27]. The conditions in Tables 2–4 correspond to the operating conditions under which the process simulation was carried out.

The mathematical method we used to find the convergence of the simulation process was Newton's Method [28,29], for which a maximum of 100 iterations was established.

2.4. Sensitivity analysis

Sensitivity analysis was conducted in DWSIM 8.6.7 with the tool "Sensitivity Study" to determine the input and output selection in an Artificial Neural Network (ANN) to evaluate the relative importance of variables. It aids in of identifying the most relevant features while eliminating irrelevant ones, optimizing the architecture, and diagnosing potential issues. In order to carry out this analysis, the potential manipulated variables were defined, establishing variation ranges in accordance with the physical-chemical logic of the actual process.

2.5. Design and training of the ANN

The ANN training adjusts the weights of the connections between neurons for the ANN to make adequate predictions regarding the targeted output data. Validation measures the ANN's prediction

errors to assess its performance. The testing process evaluates the prediction of ANN using pairs of data not used in the training process [24].

Based on the guidelines of Chen et al. [30], 70% of the entire dataset (175 data sets) were employed for ANN learning and training, while the remaining 30% (75 data sets) were dedicated to testing to evaluate the ANN learning proficiency.

The literature relevant to ANNs recommends utilizing a minimum of 50 data points for predictive regression algorithms [31–33]. In line with this guidance, 250 data pairs were generated by introducing random variations to the operational parameters and/or performance indicators selected for this investigation.

2.6. ANN validation

In the validation of the ANN, we applied the following performance metrics: mean square error (MSE) and regression coefficient (R), as defined by Eqs (1) and (2), respectively, and also employed ANOVA. Furthermore, we fine-tuned the ANN's performance through an iterative process to minimize MSE and enhance correlation coefficients during the training, validation, and testing phases.

$$MSE = \frac{1}{n}\sum_{t=1}^{n}\left(y - y'\right)^2 \tag{1}$$

$$R = \frac{n\sum_{i=1}^{n}(y'y) - [\sum_{i=1}^{n} y'][\sum_{i=1}^{n} y]}{\sqrt{[n\sum_{i=1}^{n} y^2 - [\sum_{i=1}^{n} y^2][n\sum_{i=1}^{n} y'^2 - [\sum_{i=1}^{n} y'^2]}} \tag{2}$$

where n is the number of observations, y are the actual results (simulation outputs), and y' are the predicted targets (ANN outputs).

3. Results and discussion

This section presents the analysis and discussion of the process simulation and the ANN's design, training, and validation.

3.1. Simulation validation

The simulation process in DWSIM was validated by comparing it to a study done in ASPEN PLUS by Feng et al. [1]. Table 5 shows the percentage errors for the mole fractions of key components in the distillation columns, which were less than 4%. This small percentage of error is explained by the presence of tiny amounts of other substances in the distillate and bottom streams, which are considered negligible.

Table 5. Simulation validation (mole fraction).

Column	Parameter	Aspen Plus Feng et al. [1]	DWSIM	Error (%)
Extractive (EDC)	n-hexane distillate	0.999	0.991	0.80
	NMP bottom	0.715	0.691	3.35
Recovery (ERC)	EA distillate	0.999	0.999	0
	NMP bottom	0.999	0.964	3.63

3.2. Sensitivity analysis

The critical variables affecting the products of interest were selected when modified in the extractive distillation and solvent recovery stages. The sensitivity analyses carried out for the selection of the variables which significantly impacted to the target compounds are further detailed in Appendix A.

It is crucial to highlight that the choice of input variables for the ANN was grounded in their substantial impact, influencing the composition of n-hexane and ethyl acetate by more than 10%. Additionally, we emphasize the consideration of variables previously investigated in studies about distillation processes [34–36]. Table 6 shows the parameters that directly influenced the obtainment of high-purity components.

Table 6. ANN inputs and outputs.

ANN	Column	Nomenclature	Parameter	Units
Inputs	Extractive (EDC)	T1-F	Feed flow inlet temperature	℃
		FM1-F	Feed Stream Mass Flow	kg/h
		FM2-MU	Make-up stream mass flow	kg/h
	Recovery (ERC)	RR-ERC	ERC tower reflux ratio	-
Outputs	Extractive (EDC)	X_{HE}-EDC	Mole fraction of n-hexane in the distillate of EDC	-
		X_{NMP}-EDC	Mole fraction of N-methyl-2 pyrrolidone in the bottom of EDC	-
	Recovery (ERC)	X_{EA}-ERC	Mole fraction of ethyl acetate in the distillate of ERC	-
		X_{NMP}-ERC	Mole fraction of N-methyl-2 pyrrolidone in the bottom of ERC	-

Table 7 shows the range of variation of the inputs chosen based on typical and extreme ranges of operation.

Table 7. ANN input's restrictions.

Column	Parameter	Nomenclature	Range	Units
Extractive (EDC)	Feed flow inlet temperature	T1-F	20–150	℃
	Feed Stream Mass Flow	FM1-F	3–100	kg/h
	Make-up stream mass flow	FM2-MU	8000–10000	kg/h
Recovery (ERC)	ERC tower reflux ratio	RR-ERC	0.8–2	-

3.3. Design and training of the ANN

The ANN design (Figure 3) is based on four input parameters: Feed flow inlet (T1-F), Feed Stream Mass Flow temperature pressure (FM1-F), Make-up stream mass flow (FM2-MU), and ERC tower reflux ratio (RR-ERC). These inputs were selected based on a sensitivity analysis, which identified the processing parameters that had the most substantial impact on the critical quality of the final product. Four outputs parameters were considered: Mole fraction of n-hexane in the distillate of EDC (X_{HE}-EDC), Mole fraction of N-methyl-2 pyrrolidone in the bottom of EDC (X_{NMP}-EDC), Mole fraction of ethyl acetate in the distillate of ERC (X_{EA}-ERC), and Mole fraction of N-methyl-2

pyrrolidone in the bottom of ERC (X_{NMP}-ERC). Figures 4 and 5 describe the inputs and outputs used in the ANN design (Appendix B).

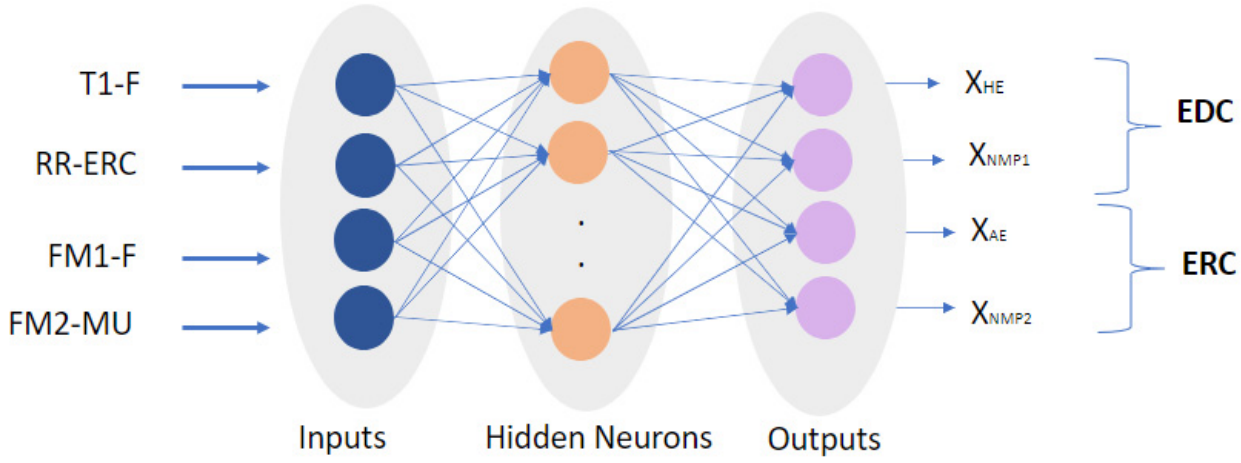

Figure 3. Schematic of the designed ANN.

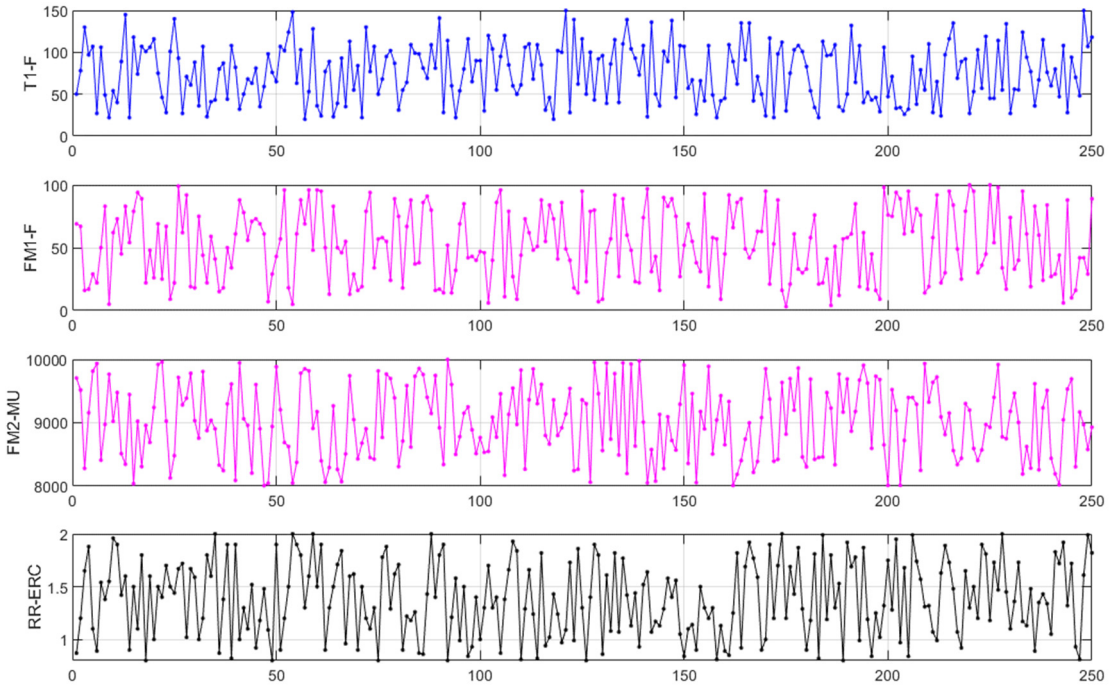

Figure 4. ANN's inputs.

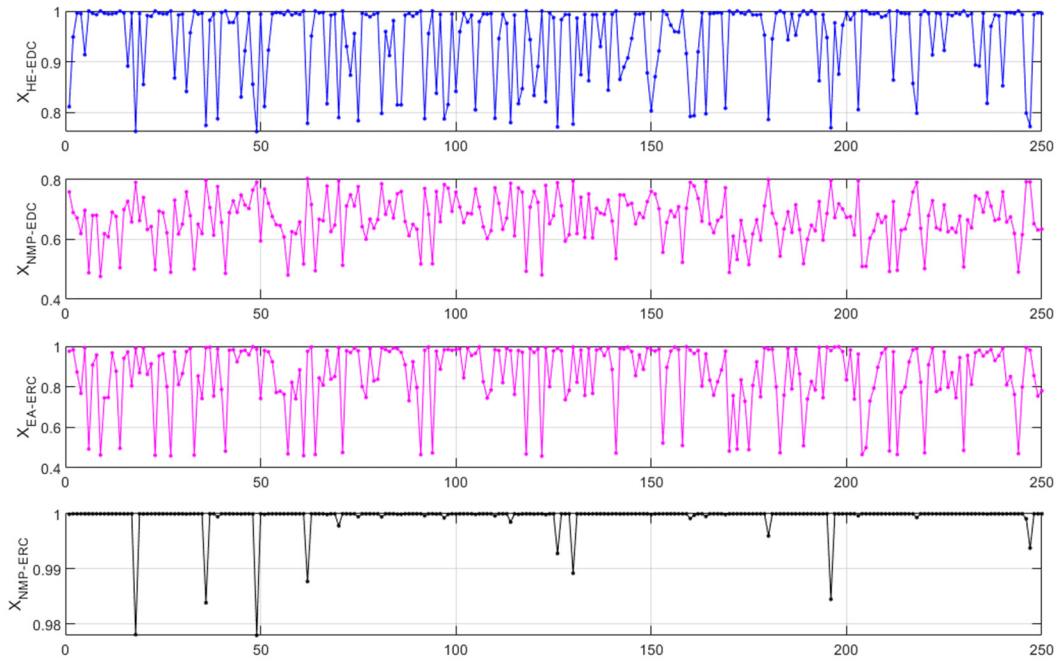

Figure 5. ANN's outputs.

3.4. ANN topology

This section describes the design and structuring of the ANN by analyzing the correlation coefficient (R) and the mean square error (MSE).

3.4.1. Selection of ANN training algorithm

The ANN architecture developed in this work utilized three training algorithms that have been shown in previous studies to effectively minimize the mean squared error (MSE) loss function: The Levenberg-Marquardt (LM), Bayesian regularization (BR), and scaled conjugate gradient back-propagation (SCG) algorithms. These training methods outperform many other commonly used algorithms by more effectively converging towards solutions with lower MSE values, according to the body of literature on neural network optimization approaches [37–39].

Similar to other predictive modeling studies [40–44], the performance of the three training algorithms was evaluated by examining the coefficient of determination (R) and mean squared error (MSE) metrics (Table 8). The number of neurons in the hidden layer was systematically varied to evaluate how this architectural choice impacted model accuracy across the different optimization approaches. This enables comparison of the algorithms' robustness and sensitivity to tuning parameters.

Table 8. Pearson's correlation coefficient (*R*) and mean square error (MSE) values for trial and error using Levenberg-Marquardt (LM), Bayesian regularization (BR), and scaled conjugate gradient back-propagation (SCG) algorithms.

#hidden neurons	LM		BR		SCG	
	R Global	*MSE*	*R* Global	*MSE*	*R* Global	*MSE*
20	0.9855	0.0008	0.9899	0.0006	0.9547	0.0029
40	0.8721	0.0337	0.9658	0.0001	0.8617	0.0349
60	0.9507	0.0286	0.9862	1.36×10^{-6}	0.9208	0.0370
80	0.9300	0.0237	0.9939	2.56×10^{-7}	0.7676	0.0756
100	0.8916	0.0488	0.9902	7.12×10^{-7}	0.9356	0.0352

The results of the training process detailed in Table 7 demonstrate that the Bayesian regularization (BR) algorithm yielded the most accurate and reliable model for predicting the target outputs, with the minimum mean squared error (MSE) of 2.56×10^{-7} and maximum R-value of 0.9939. Previous studies have highlighted the strengths of BR algorithm to discovering complex relationships in the data and generating less biased predictions [37,45,46].

Although computationally more expensive than other techniques, BR has been shown to generate robust generalizations from small, noisy, or complex datasets, outperforming methods like Levenberg-Marquardt. This strength in modeling potential nonlinear effects, even with limited data samples, makes BR well-suited for quantitative analyses requiring accurate and dependable predictive performance [37]. By leveraging BR's capabilities, the developed model provides a solid foundation for drawing insights from the empirical data collected.

Beyond performance in the training stage, the choice was also based on the BR algorithm's ability to avoid overfitting, a common problem in complex predictive models. The fitting parameters of the BR algorithm are limited by a regularization term, converting a non-linear problem into a statistical one through regressions, thus allowing better model fitting and prediction [47,48]. Also, it is essential to indicate that Bayesian regression, in contrast to other models, simplifies the optimization of the system, which will subsequently facilitate the energy optimization of the process [49] .

3.4.2. Selection of the number of neurons in the hidden layer

Determining the optimal neuron's number is useful to conduct trials in determining the required local minimum in the error surface, and oscillations in *R* [2].

The analysis in Table 9 shows that 20 and 80 neurons yield the greatest R-values in the testing phase. When 20 neurons were used, the R-value in testing reached 0.9574, while the R-value with 80 neurons was 0.9618. Furthermore, the MSE values were 0.0006 with 20 neurons and 2.26×10^{-7} with 80 neurons. Based on the maximum R-value and minimum MSE, these results suggest that 80 is the optimal quantity of neurons for this hidden layer. The higher R, along with the lower error with 80 neurons, indicates it provided the best model performance.

The ANN model developed in this work constructed with MATLAB NNTOOL R2018a. Based on the analysis, the ANN structure contains four input neurons, a single hidden layer with 80 neurons as determined optimal, and four output neurons. As noted in previous predictive modeling researches, implementing one hidden layer is often sufficient for enabling accurate forecasts across a wide range of ANN applications [24,50].

Table 9. *R* and *MSE* values for determining the optimal number of neurons in the hidden layer using Bayesian regularization algorithm.

# hidden neurons	*R* Training	*R* Testing	*R* Global	*MSE*
20	0.9963	0.9574	0.9899	0.0006
40	0.9991	0.8265	0.9658	0.0001
60	0.9999	0.9137	0.9862	1.36×10^{-6}
80	0.9999	0.9618	0.9939	2.26×10^{-7}
100	0.9999	0.9242	0.9902	7.12×10^{-7}

3.4.3. ANN training and testing

Table 10 illustrates MSE values for the artificial neural network (ANN) training and testing phases. Validation phase results are not included, as ANNs utilizing Bayesian regularization (BR) can minimize the need for validation by leveraging that data to produce more robust models during training. The low MSE scores of 2.56×10^{-7} for training and 0.0020 for testing show that the ANN makes accurate predictions. Figure 6 illustrates the MSE progression across both phases. The MSE of the training data decreases towards zero, signaling the ANN's strong predictive abilities.

Figure 7 shows R values for both the training and testing phases. The R-values are 0.999 for training and 0.961 for testing, while the overall R-value is 0.993. These high R-values signify an acceptable correlation between outputs and targets. In general, R-values approaching 1 indicate better ANN performance. To validate the ANN, R-values ranging from 0.97 to 1 and MSE below 0.0025 were set as benchmarks. Based on meeting these criteria, the developed ANN can be considered an accurate and reliable predictive model for this application.

Table 10. Mean square error of ANN designed.

PHASE	MSE
trainPerfomance (training)	2.56×10^{-7}
testPerfomance (testing)	0.0020

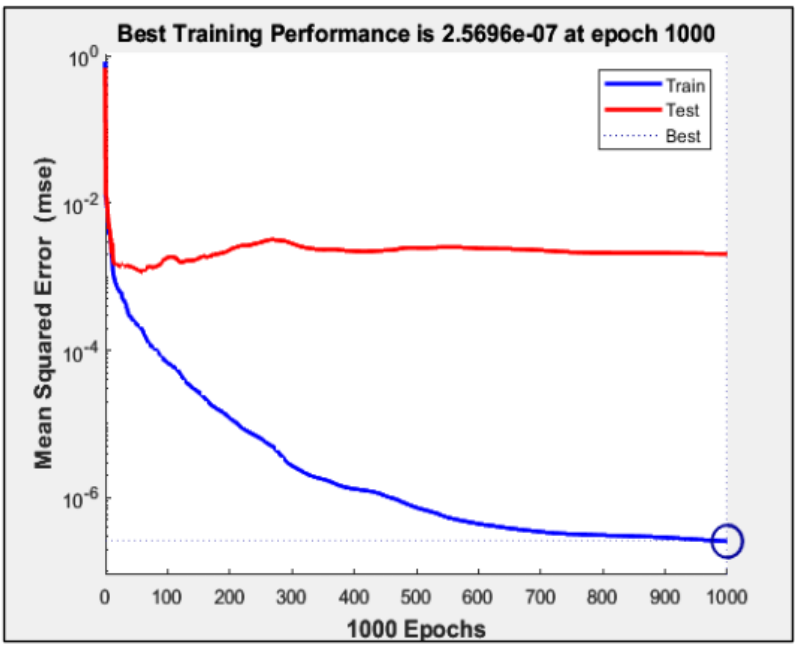

Figure 6. ANN training performance (MSE).

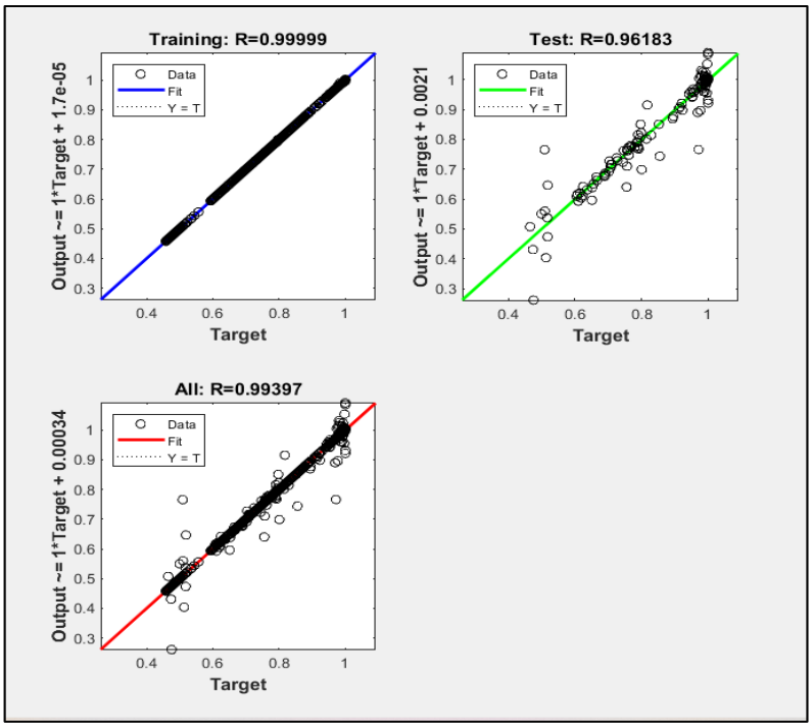

Figure 7. Regression coefficient *R* for the ANN.

3.5. Model prediction of X_{HE} , X_{NMP} in the extractive column (EDC), and X_{EA} y X_{NMP} in the recovery column(ERC)

Figures 8–11 illustrate the overlap between the experimentally obtained simulation values and the ANN model predictions for the extractive and recovery columns, respectively. The comparative results across both columns demonstrate a high degree of parity. Through effectively approximating the observational simulation data, the developed ANN model proves its robustness and suitability for forecasting X_{HE}, X_{NMP} and X_{EA} under conditions utilizing N-methyl-2-pyrrolidone for n-hexane and ethyl acetate separations. Close conformance between experimental outputs and AI-generated outputs substantiates the modeling framework for application within this specific solvent extraction process.

Based on the analysis of Figures 8–11, the average percentage errors (%E) of the predictions are: 0.572% (X_{HE} in the distillate) and 0.867% (X_{NMP} in the bottom) in the extractive column (EDC); and 1.313% (X_{EA} in the distillate) and 0.069% (X_{NMP} in the bottom) in the recovery column (ERC).

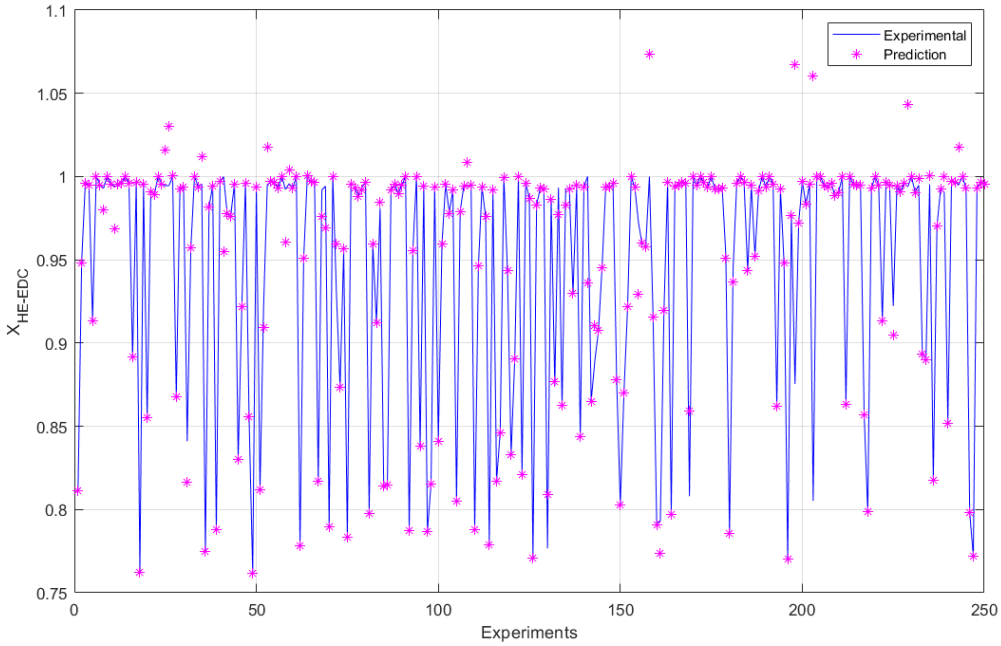

Figure 8. DWSIM (Experimental) and ANN (prediction) results in EDC distillate (X_{HE}).

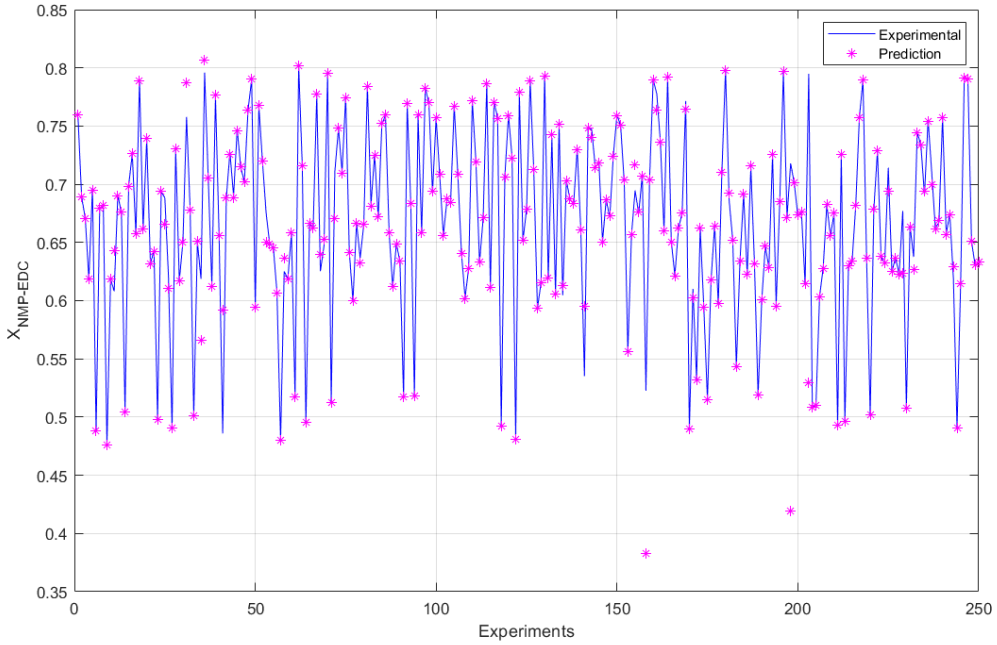

Figure 9. DWSIM (Experimental) and ANN (prediction) results in EDC bottoms (X_{NMP}).

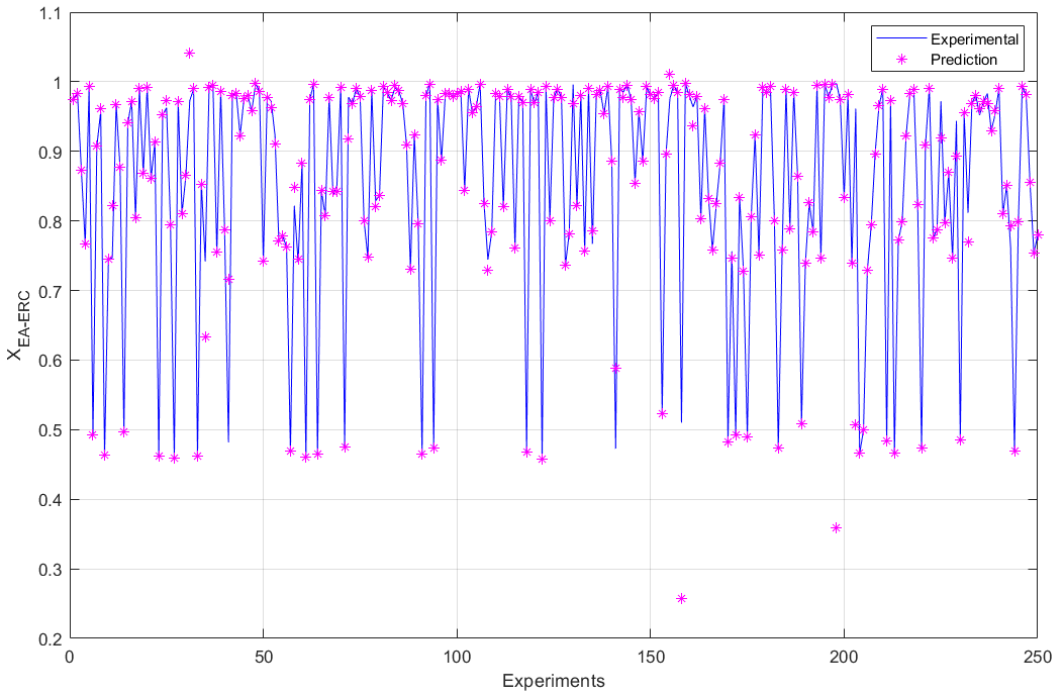

Figure 10. DWSIM (Experimental) and ANN (prediction) results in ERC distillate (X_{EA}).

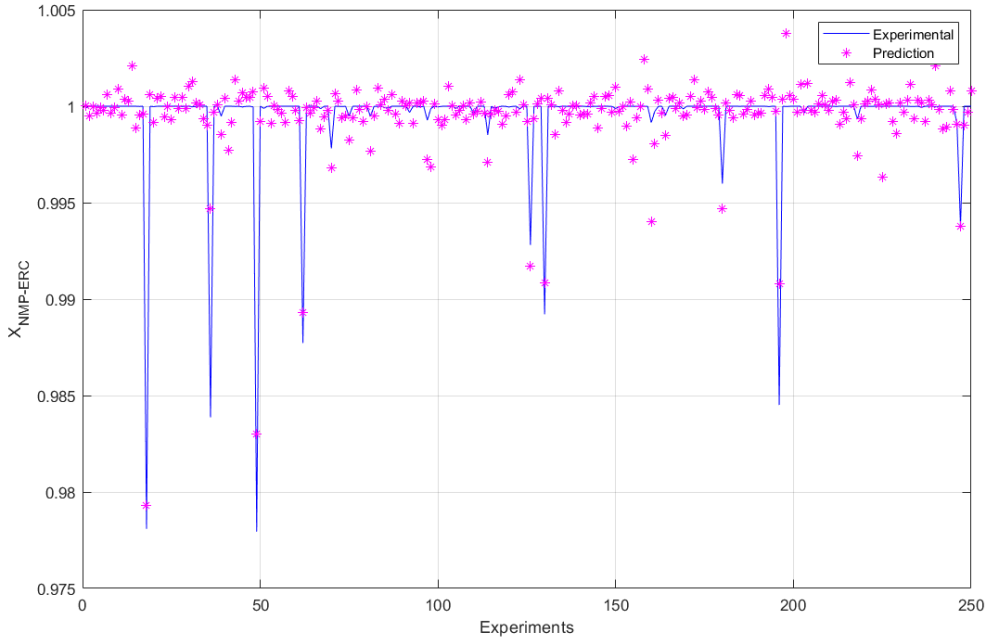

Figure 11. DWSIM (Experimental) and ANN (prediction) results in ERC bottoms (X_{NMP}).

3.6. Analysis of ethyl acetate (EA), N-hexane (HE), and NMP concentrations of the system

The analysis of the ANN inputs has been carried out to identify the operating conditions that lead to the optimal points of the system. In this context, the optimal points regarding n-hexane, ethyl acetate, and NMP concentrations are defined. The analysis results are detailed in Table 11, describing the operating parameters associated with the maximum concentrations of the compounds of interest.

Table 11. Maximum concentration of the compounds of interest (X_{HE}, X_{NMP} and X_{EA}).

Experiment	Feed flow inlet (T1-F),	Feed Stream Mass Flow (FM1-F)	Make-up stream mass flow (FM2-MU)	ERC tower reflux ratio (RR-ERC)	Distillate of EDC (X_{HE}-EDC)	Bottom of EDC (X_{NMP}-EDC)	Distillate of ERC (X_{EA}-ERC)
6	27	0.89	9935	22	1.0000	0.4881	0.4925
9	22	1.55	9766	5	1.0000	0.4760	0.4632
14	22	0.9	9446	54	1.0000	0.5047	0.4967
23	28	1.7	9025	67	1.0000	0.4986	0.4618
27	27	1.72	9281	62	1.0000	0.4898	0.4591
33	23	1.8	8876	22	1.0000	0.5005	0.4624
41	32	1	9948	88	1.0000	0.4860	0.4818
57	20	1.3	9852	69	1.0000	0.4804	0.4687
61	24	1.9	8398	95	1.0000	0.5174	0.4599
62	77	0.9	8059	50	0.7781	0.8019	0.9749
64	23	1.5	9267	83	1.0000	0.4950	0.4656
71	22	1.5	8677	19	1.0000	0.5131	0.4756
91	28	1.9	8341	14	1.0000	0.5171	0.4652
94	22	1.58	8500	32	1.0000	0.5180	0.4736
122	28	1.73	9541	40	1.0000	0.4808	0.4576
141	23	1.64	8049	97	1.0000	0.5352	0.4728
153	26	0.9	8054	38	1.0000	0.5563	0.5226
158	22	0.81	9042	57	1.0000	0.5226	0.5102
159	42	1.13	9427	9	0.9160	0.7035	0.9975
172	22	1.2	8391	53	1.0000	0.5323	0.4925
175	30	1.2	8818	3	1.0000	0.5152	0.4894

Table 11 shows that the maximum fraction of n-hexane in the distillate of the EDC column has been achieved under various operating conditions. However, the maximum concentration of NMP in the EDC was obtained in experiment 62 (yellow light shading), characterized by a Feed flow inlet (T1-F) of 77 °C, a Feed Stream Mass Flow (FM1-F) = 0.9 kg/h, a Make-up stream mass flow (FM2-MU) = 8059 kg/h, and an ERC tower reflux ratio (RR-ERC) = 50.

Finally, it should be noted that the maximum concentration of ethyl acetate was reached in experiment 159 (green shading), where the operating conditions were as follows: T1-F = 42 °C, FM1-F = 1.13, FM2-MU = 9427 kg/h, and RR-ERC = 9. This detailed analysis provides an understanding of the operating conditions that maximize the concentrations of the compounds of interest in the system.

However, it is imperative to recognize that the successful implementation of ANN in a plant environment has certain limitations. An extensive historical database is required to implement it effectively, serving as a basis for retroactive and adaptive learning of already trained ANNs. That is why it is essential to have detailed records and representatives of past operations. Furthermore, an automatic monitoring and control system is another critical factor. The energy and environmental optimization that can be developed in the plant through the ANNs intrinsically depends on the system's ability to react in real-time to the variable conditions of the plant, thus ensuring the effective implementation of the optimal strategies derived from the ANNs. These fundamental elements are necessary for the ANN's ability to contribute to operational efficiency and sustainability to be expanded meaningfully.

In future studies, energy and environmental parameters will be considered for a hybrid optimization combining genetic optimization algorithms with ANN. Hybrid methods incorporate aspects of other design approaches, such as leveraging thorough simulation to produce training data for an artificial intelligence model or utilizing a heuristic optimization technique to refine the outputs of a mathematical optimization method [34,51].

3.7. ANN model verification

The ANN predictive capacity of the X_{HE}, X_{NMP} and X_{EA} in the EDC and ERC was verified with a set of 50 random input data (Feed flow inlet (T1-F), Feed Stream Mass Flow temperature pressure (FM1-F), Make-up stream mass flow (FM2-MU) and ERC tower reflux ratio (RR-ERC)) unknown by the ANN. The results show an overlap between the experimental data and the predictions. This indicates that ANN has a good predictive capacity for the mole fractions of distillates and residues of the distillation columns (Figure 12).

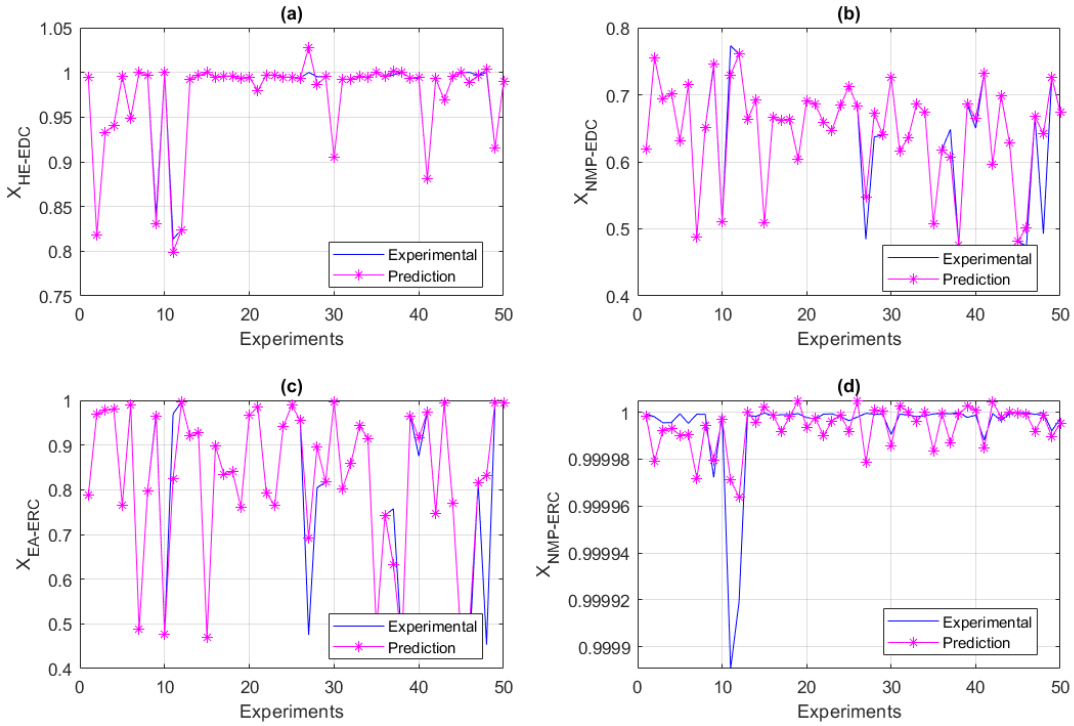

Figure 12. Comparison between experimentals and predictions datas-EDC: a) X_{HE} (distillate), b) X_{NMP} (bottoms) and ERC: c) X_{EA} (distillate), d) X_{NMP} (bottoms).

Table 12. ANOVA.

Source	Sum of squares	DOF	Mean square	F-value	P-value
X_{HE} in EDC distillate					
Inter groups	5.34×10^{-7}	1	5.34×10^{-7}	0.00	0.00
Intra groups	0.2682	98	0.0027		
Total (Corr.)	0.2682	99			
X_{NMP} in EDC bottoms.					
Inter groups	0.0004	1	0.0004	0.07	0.07
Intra groups	0.5995	98	0.0061		
Total (Corr.)	0.6000	99			
X_{EA} in ERC distillate					
Inter groups	0.0025	1	0.0025	0.08	0.08
Intra groups	3.0739	98	0.0313		
Total (Corr.)	3.0764	99			
X_{NMP} in ERC bottoms					
Inter groups	4.04×10^{-11}	1	4.04×10^{-11}	0.19	0.19
Intra groups	2.05×10^{-8}	98	2.09×10^{-10}		
Total (Corr.)	2.05×10^{-8}	99			

In this research we used the functions ANOVA [52] using SPSS 22.0 to validate the ANN statistically. Table 12 shows the results from ANOVA and, for all cases, P-values (probability value in statistical significance tests) are greater than 0.05, indicating no statistically significant differences between the means of the observations and the predictions. This statistical test reveal that the ANN constructed is statistically valid for predicting X_{HE}, X_{NMP} and X_{EA} in the EDC and ERC, with a confidence level of 95%.

3.8. Recommended steps for ANN implementation

Figure 13 presents a generalized diagram of the steps and actions necessary for the implementation of the ANN in the industrial process. The following recommendations are suggested for implementing ANN in real-time: Define the objectives of the ANN (Quality Control or Process Optimization); define the historical database for re-training the ANN, preprocess the database, train the ANN, implement the ANN in hardware integrated into the automatic process control system, implement real-time ANN performance monitoring mechanisms, periodically update the ANN through feedback loops for continuous improvement of the ANN, implement security measures based on the predictions made by the ANN, and document the entire process.

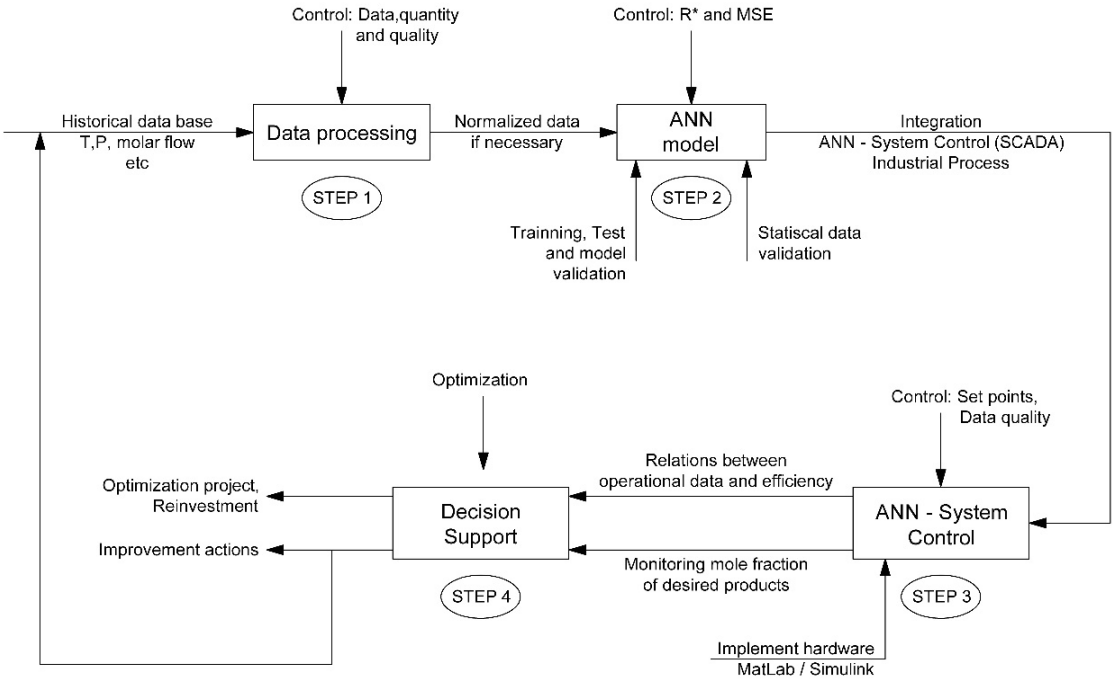

Figure 13. Generalized diagram to implement the ANN.

3.9. Potential challenges in implementing the ANN

Implementing ANN in a industrial plants faces challenges that can influence its performance and effectiveness in real-world environments. A brief description of each of these challenges is given below:

Adapt the parameters and architecture of the ANN to the specific conditions of each extractive distillation plant: The designed ANN was trained on a simulator data set, but compositions and conditions may vary in large-scale industrial environments. It is essential to use the historical database (pressures, temperatures, molar flows, recirculation rates, quality of obtained products,

among others) available on-site from those environments, and the ANN must be partially retrained to achieve optimal performance. However, obtaining sufficient, high-quality, labeled data can be expensive, time-consuming, and challenging [53].

Integrate ANN predictions into these industrial plants' existing monitoring and control systems: Once the ANN has been validated in the plant, one of the main advantages of the scaling process is its ability to accurately estimate the system's behavior when changes occur in operational variables or when a disturbance is introduced into the system [54–56]. However, this requires a communication interface (Hardware) between the ANN and the closed-loop controllers of the plant or SCADA system that guarantees the reliability and inference speed of the ANN. Hardware implementations (HW) are challenging but yield good performance. Digital architectures offer high flexibility, accuracy, replicability, low noise sensitivity, testability, and no-weight storage issues. With an effective integration between the SCADA and the ANN, the operational efficiency of the ANN would improve in real-time, allowing adequate adjustments against disturbances that could affect the quality of the mole fractions of the desired compounds at the exit of the distillation towers. The Field Programmable Gate Array (FPGA) is viable for achieving high control performance and state reconstruction in industrial control applications; it offers a range of benefits, such as the ability to implement highly parallel arithmetic architectures, programmable hardwired features, fast time-to-market, shorter design cycles, embedded processors, low power consumption, and higher density for digital system implementation [57].

Computational requirements: The training and validation of an industrial plant requires a significant amount of computational resources. ANN requires a computer system with sufficient processing power, including a high-end CPU, graphics processing unit (GPU), FPGA, or distributed computing systems. It requires adequate memory and robust network infrastructure to handle large data sets, either storing them locally or accessing them over an efficient storage network (big cloud) [58]. Furthermore, since industrial data is confidential, it is essential to implement appropriate security and privacy measures to protect data confidentiality during the ANN implementation process.

4. Conclusions

The mole fractions of an alternative extractive distillation system for separating C_6H_{14}-$C_4H_8O_2$ using C_6H_7NO as solvent were predicted using an ANN based on the process simulation in DWSIM. The ANN developed has 80 hidden neurons and was trained with a base of 250 pairs of data with four input variables (neurons): Feed flow inlet (T1-F), Feed Stream Mass Flow temperature pressure (FM1-F), Make-up stream mass flow (FM2-MU) and ERC tower reflux ratio (RR-ERC). It is capable of predicting four output variables (neurons): Mole fraction of n-hexane in the distillate of EDC (X_{HE}-EDC), Mole fraction of N-methyl-2 pyrrolidone in the bottom of EDC (X_{NMP}-EDC), Mole fraction of ethyl acetate in the distillate of ERC (X_{EA}-ERC), and Mole fraction of N-methyl-2 pyrrolidone in the bottom of ERC (X_{NMP}-ERC).

The Bayesian regularization approach was used to train the ANN, which has an *MSE test* performance of 0.0020 and a test *R* of 0.9618. A comparison statistical analysis (ANOVA) between the data (DWSIM) and the values predicted by the neural network was also used to validate the ANN. Statistical tests show that the ANN accurately predicts the mole fractions at the outputs with a 95% significance level.

The results suggest that the artificial neural network (ANN) developed in this research holds potential as a predictive analytics tool for improving the efficiency of separating solvent mixtures containing ethyl acetate and n-hexane. These particular organic solvents play a significant role in

chemical and pharmaceutical manufacturing. To utilize the ANN effectively, it is essential to input the actual operational parameters of the described process, implement them in real-time, and validate the predictions at the control points determined by the ANN.

To implement ANN in real-time, the following recommendations are suggested: clearly define the objectives of the ANN, establish a historical database for re-training, preprocess the database, train the ANN, integrate the hardware into the automatic process control system, monitor the performance of the ANN in real-time, continuously update the ANN through feedback loops, implement security measures based on ANN predictions, and thoroughly document the entire process.

The implementation of ANN in an industrial process faces several challenges, among which the most important are: Adapt the parameters and architecture of the ANN to the specific conditions of each extractive distillation plant, Integrate the ANN predictions into monitoring existing industrial plants and control systems, and Computational requirements.

In future research, efficient and low computational cost strategies will be sought for the real-time implementation of the ANN. In addition, the application of genetic optimization algorithms to ANNs will be explored using hybrid approaches, especially considering energy efficiency and environmental impact parameters.

Use of AI tools declaration

The authors declare that they have not used Artificial Intelligence (AI) tools in the creation of this article.

Acknowledgments

The authors thank the Security Research Group on Environment and Engineering, "GISAI" for allowing the execution of this research.

Conflict of interest

There is no conflict of interest.

Supplementary

Appendix A and Appendix B.

References

1. Feng ZF, Shen WF, Rangaiah GP, et al. (2020) Design and control of vapor recompression assisted extractive distillation for separating n-hexane and ethyl acetate. *Sep Purif Technol* 240: 116655. https://doi.org/10.1016/j.seppur.2020.116655
2. Acosta J, Arce A, Martínez-Ageitos J, et al. (2002) Vapor-Liquid equilibrium of the ternary system ethyl Acetate+ Hexane+ acetone at 101.32 kPa. *J Chem Eng Data* 47: 849–854. https://doi.org/10.1021/je0102917
3. Yang Kong Z, Yeh Lee H, Sunarso J (2022) The evolution of process design and control for ternary azeotropic separation: Recent advances in distillation and future directions. *Sep Purif Technol* 284: 120292. https://doi.org/10.1016/j.seppur.2021.120292

4. Gerbaud V, Rodriguez-Donis I, Hegely L, et al. (2019) Review of extractive distillation. Process design, operation, optimization and control. *Chem Eng Res Des* 141: 229–271. https://doi.org/10.1016/j.cherd.2018.09.020
5. Iqbal A, Akhlaq Ahmad S, Ojasvi (2019) Design and control of an energy-efficient alternative process for separation of dichloromethane-methanol binary azeotropic mixture. *Sep Purif Technol* 219: 137–149. https://doi.org/10.1016/j.seppur.2019.03.005
6. Zhu Z, Yu X, Ma Y, et al. (2020) Efficient extractive distillation design for separating binary azeotrope via thermodynamic and dynamic analyses. *Sep Purif Technol* 238: 116425. https://doi.org/10.1016/j.seppur.2019.116425
7. Yang X, Ward J (2018) Design of a pressure-swing distillation process for the separation of n-hexane and ethyl acetate using simulated annealing. *Comp Aid Chem Eng* 44: 121–126. https://doi.org/10.1016/B978-0-444-64241-7.50015-X
8. Lü L, Zhu L, Liu H, et al. (2018) Comparison of continuous homogenous azeotropic and pressure-swing distillation for a minimum azeotropic system ethyl acetate/n-hexane separation. *Chin J Chem Eng* 26: 2023–2033. https://doi.org/10.1016/j.cjche.2018.02.002
9. Li Y, Sun T, Ye Q, et al. (2021) Investigation on energy-efficient extractive distillation for the recovery of ethyl acetate and 1,4-dioxane from industrial effluent. *J Clean Prod* 329: 129759. https://doi.org/10.1016/j.jclepro.2021.129759
10. Shi F, Gao J, Huang X (2016) An affine invariant approach for dense wide baseline image matching. *Int J Distrib Sens Netw,* 12. https://doi.org/10.1177/1550147716680826
11. Sun L, Liang F, Cui W (2021) Artificial neural network and its application research progress in chemical process. *Asian J Res Comput Sci* 12: 177–185. https://doi.org/10.9734/ajrcos/2021/v12i430302
12. Singh RP, Heldman DR (2008) Introduction to food engineering. *A volume in Food science and technology,* Fifth Eds., California: Academic Press. Available from: https://www.sciencedirect.com/book/9780123985309/introduction-to-food-engineering.
13. Elgibaly A, Ghareeb M, Kamel S, et al. (2021) Prediction of gas-lift performance using neural network analysis. *AIMS Energy* 9: 355–378. https://doi.org/10.3934/energy.2021019
14. Kandil A, Khaled S, Elfakharany T (2023) Prediction of the equivalent circulation density using machine learning algorithms based on real-time data. *AIMS Energy* 11: 425–453. https://doi.org/10.3934/energy.2023023
15. Hamdi M, El Salmawy H, Ragab R (2023) Optimum configuration of a dispatchable hybrid renewable energy plant using artificial neural networks: Case study of Ras Ghareb, Egypt. *AIMS Energy* 11: 171–196. https://doi.org/10.3934/energy.2023010
16. Aly A, Saleh B, Bassuoni M, et al. (2019) Artificial neural network model for performance evaluation of an integrated desiccant air conditioning system activated by solar energy. *AIMS Energy* 7: 395–412. https://doi.org/10.3934/energy.2019.3.395
17. Zhang Z, Zhao J (2017) A deep belief network based fault diagnosis model for complex chemical processes. *Comput Chem Eng* 107: 395–407. https://doi.org/10.1016/j.compchemeng.2017.02.041
18. Yazdizadeh M, Jafari Nasr M, Safekordi A (2016) A new catalyst for the production of furfural from bagasse. *RSC Adv* 61: 55778–55785. https://doi.org/10.1039/c6ra10499a
19. Esonye C, Dominic Onukwuli O, Uwaoma Ofoefule A (2019) Optimization of methyl ester production from Prunus amygdalus seed oil using response surface methodology and artificial neural networks. *Renewable Energy* 130: 61–72. https://doi.org/10.1016/j.renene.2018.06.036

20. Ge X, Wang B, Yang X, et al. (2021) Fault detection and diagnosis for reactive distillation based on convolutional neural network. *Comput Chem Eng* 145: 107172. https://doi.org/10.1016/j.compchemeng.2020.107172
21. de Araújo Neto AP, Sales FA, Brito RP (2021) Controllability comparison for extractive dividing-wall columns: ANN-based intelligent control system versus conventional control system. *Chem Eng Proc Intens* 160: 108271. https://doi.org/10.1016/j.cep.2020.108271
22. Inyang V, Lokhat D (2022) Propionic acid recovery from dilute aqueous solution by emulsion liquid membrane (ELM) technique: optimization using response surface methodology (RSM) and artificial neural network (ANN) experimental design. *Sep Scie Tech* 57: 284–300. https://doi.org/10.1080/01496395.2021.1890774
23. DWSIM (2020) DWSIM—The open source chemical process simulator. Available from: https://dwsim.org.
24. Chuquin-Vasco D, Parra F, Chuquin-Vasco N, et al. (2021) Prediction of methanol production in a carbon dioxide hydrogenation plant using neural networks. *Energies* 14: 1–18. https://doi.org/10.3390/en14133965
25. Dimian AC, Bildea CS, Kiss AA (2014) Introduction in process simulation. *Comput Aided Chem Eng* 35: 35–71. https://doi.org/10.1016/B978-0-444-62700-1.00002-4
26. Kiss AA (2013) Advanced distillation technologies: Design, control and applications. 1 Eds., Noida, India:Wiley. https://doi.org/10.1002/9781118543702
27. Soave G, Gamba S, Pellegrini L (2010) SRK equation of state: predicting binary interaction parameters of hydrocarbons and related compounds. *Fluid Phase* 299: 285–293. https://doi.org/10.1016/j.fluid.2010.09.012
28. Hu Y, Wang J, Tan C, et al. (2017) Further improvement of fluidized bed models by incorporating zone method with Aspen Plus interface. *Energy Proc* 105: 1895–1901. https://doi.org/10.1016/j.egypro.2017.03.556
29. Mlazi NJ, Mayengo M, Lyakurwa G, et al. (2024) Mathematical modeling and extraction of parameters of solar photovoltaic module based on modified Newton-Raphson method. *Results Phys* 57: 107364. https://doi.org/10.1016/j.rinp.2024.107364
30. Chen Y, Song L, Liu Y, et al. (2020) A review of the artificial neural network models for water quality prediction. *Appl Sci* 10: 5776. https://doi.org/10.3390/app10175776
31. Singh V, Gupta I, Gupta H (2005) ANN based estimator for distillation-inferential control. *Chem Eng Proc Int* 44: 785–795. https://doi.org/10.1016/j.cep.2004.08.010
32. Pedregosa F, Varaquaux G, Gramfort A, et al. (2011) Scikit-learn:machine learning in Python. *J Mach Lear Res*. Available from: https://www.jmlr.org/papers/volume12/pedregosa11a/pedregosa11a.pdf.
33. Bloice M, Holzinger A (2016) A tutorial on machine learning and data science tools with python. *Lect Not Comp Sci* 9605: 435–480. https://doi.org/10.1007/978-3-319-50478-0_22
34. Purna Pushkala S, Panda R (2023) Design and analysis of reactive distillation for the production of isopropyl myristate. *Clean Chem Eng* 5: 100090. https://doi.org/10.1016/j.clce.2022.100090
35. Elsheikh M, Ortmanns Y, Hecht F, et al. (2023) Control of an industrial distillation column using a hybrid model with adaptation of the range of validity and an ANN-based soft sensor. *Chem Ing Tech* 95: 1114–1124. https://doi.org/10.1002/cite.202200232
36. Neves T, De Araújo Neto A, Sales F, et al. (2021) ANN-based intelligent control system for simultaneous feed disturbances rejection and product specification changes in extractive distillation process. *Sep Purif Technol* 259: 118404. https://doi.org/10.1016/j.seppur.2020.118104

37. Kayri M (2016) Predictive abilities of bayesian regularization and levenberg-marquardt algorithms in artificial neural networks: A comparative empirical study on social data. *Math Comp App* 21: 20. https://doi.org/10.3390/mca21020020
38. Bharati S, Atikur Rahman M, Podder P, et al. (2021) Comparative performance analysis of neural network base training algorithm and neuro-fuzzy system with SOM for the purpose of prediction of the features of superconductors. *Int Syst Des App* 1181: 69–79. https://doi.org/10.1007/978-3-030-49342-4_7
39. Mohan Saini L (2008) Peak load forecasting using bayesian regularization, resilient and adaptive backpropagation learning based artificial neural networks. *Elec Power Syst Res* 78: 1302–1310. https://doi.org/10.1016/j.epsr.2007.11.003
40. Wang L, Wu B, Zhu Q, et al. (2020) Forecasting monthly tourism demand using enhanced backpropagation neural network. *Neural Process Lett* 52: 2607–2636. https://doi.org/10.1007/s11063-020-10363-z
41. Zeng Y, Zeng Y, Choi B, et al. (2017) Multifactor-influenced energy consumption forecasting using enhanced back-propagation neural network. *Energy* 127: 381–396. https://doi.org/10.1016/j.energy.2017.03.094
42. Suphawan K, Chaisee K (2021) Gaussian process regression for predicting water quality index: A case study on ping river basin, thailand. *AIMS Environ Sci* 8: 268–282. https://doi.org/10.3934/environsci.2021018
43. Wang L, Wu B, Zhu Q, et al. (2020) Forecasting monthly tourism demand using enhanced backpropagation neural network. *Neural Process Lett* 52: 2607–2636. https://doi.org/10.1007/s11063-020-10363-z
44. Zhang L, Sun X, Gao S (2022) Temperature prediction and analysis based on improved GA-BP neural network. *AIMS Environ Sci* 9: 735–753. https://doi.org/10.3934/environsci.2022042
45. Suliman A, Omarov B (2018) Applying bayesian regularization for acceleration of levenberg marquardt based neural network training. *Int J Int Mult Art Inte* 5: 68. https://doi.org/10.9781/ijimai.2018.04.004
46. Garoosiha H, Ahmadi J, Bayat H (2019) The assessment of Levenberg-marquardt and bayesian Framework training algorithm for prediction of concrete shrinkage by the artificial neural network. *Cogent Eng* 6: 1609179. https://doi.org/10.1080/23311916.2019.1609179
47. Kim R, Min J, Lee J, et al. (2023) Development of bayesian regularized artificial neural network for airborne chlorides estimation. *Constr Build Mater* 383: 131361. https://doi.org/10.1016/j.conbuildmat.2023.131361
48. Yalamanchi K, Kommalapati S, Pal P, et al. (2023) Uncertainty quantification of a deep learning fuel property prediction model. *Appl Energy Comb Sci* 16: 100211. https://doi.org/10.1016/j.jaecs.2023.100211
49. Jog S, Vázquez D, Santos L, et al. (2023) Hybrid analytical surrogate-based process optimization via bayesian symbolic regression. *Comput Chem Eng* 182: 108563. https://doi.org/10.1016/j.compchemeng.2023.108563
50. Abiodun O, Jantan A, Omolara A, et al. (2018) State of the art in artificial neural network applications: A survey. *Heliyon* 4: E00938. https://doi.org/10.1016/j.heliyon.2018.e00938
51. Tgarguifa A, Bounahmidi T, Fellaou S (2020) Optimal design of the distillation process using the artificial neural networks method. *2020 1st International Conference on Innovative Research in Applied Science, Engineering and Technology (IRASET)*, Meknes, Morocco, 1–6. Available from: https://ieeexplore.ieee.org/document/9092266.

52. Kyono K, Hashimoto T, Nagai Y, et al. (2018) Analysis of endometrial microbiota by 16S ribosomal RNA gene sequencing among infertile patients: a single-center pilot study. *Reprod Med Biol* 17: 297–306. https://doi.org/10.1002/rmb2.12105
53. Talaei Khoei T, Ould Slimane H, Kaabouch N (2023) Deep learning: Systematic review, models, challenges, and research directions. *Neural Comput Appl* 35: 23103–23124. https://doi.org/10.1007/s00521-023-08957-4
54. Boger Z (1997) Experience in industrial plant model development using large-scale artificial neural networks. *Inf Sci* 101: 203–216. https://doi.org/10.1016/S0020-0255(97)00010-8
55. Acevedo L, Uche J, Del-Amo A (2018) Improving the distillate prediction of a membrane distillation unit in a trigeneration scheme by using artificial neural networks. *Water* 10: 310. https://doi.org/10.3390/w10030310
56. Shin Y, Smith R, Hwang S (2020) Development of model predictive control system using an artificial neural network: A case study with a distillation column. *J Clean Prod* 277: 124124. https://doi.org/10.1016/j.jclepro.2020.124124
57. Magdy Saady M, Hassan Essai M (2022) Hardware implementation of neural network-based engine model using FPGA. *Alex Eng J* 61: 12039–12050. https://doi.org/10.1016/j.aej.2022.05.035
58. Hasimi L, Zavantis D, Shakshuki E, et al. (2024) Cloud computing security and deep learning: An ANN approach. *Proc Comp Sci* 231: 40–47. https://doi.org/10.1016/j.procs.2023.12.155

AIMS Press